

Combustion characteristics and emissions of 2-methylfuran compared to 2,5-dimethylfuran, gasoline and ethanol in a DISI engine

Wang, Chongming; Xu, Hongming; Daniel, Ritchie; Ghafourian, Akbar; Herreros, Jose; Shuai, Shijin; Ma, Xiao

DOI:

[10.1016/j.fuel.2012.05.043](https://doi.org/10.1016/j.fuel.2012.05.043)

License:

Creative Commons: Attribution-NonCommercial-NoDerivs (CC BY-NC-ND)

Citation for published version (Harvard):

Wang, C, Xu, H, Daniel, R, Ghafourian, A, Herreros, J, Shuai, S & Ma, X 2013, 'Combustion characteristics and emissions of 2-methylfuran compared to 2,5-dimethylfuran, gasoline and ethanol in a DISI engine', *Fuel*, vol. 103, pp. 200-211. <https://doi.org/10.1016/j.fuel.2012.05.043>

[Link to publication on Research at Birmingham portal](#)

General rights

Unless a licence is specified above, all rights (including copyright and moral rights) in this document are retained by the authors and/or the copyright holders. The express permission of the copyright holder must be obtained for any use of this material other than for purposes permitted by law.

- Users may freely distribute the URL that is used to identify this publication.
- Users may download and/or print one copy of the publication from the University of Birmingham research portal for the purpose of private study or non-commercial research.
- User may use extracts from the document in line with the concept of 'fair dealing' under the Copyright, Designs and Patents Act 1988 (?)
- Users may not further distribute the material nor use it for the purposes of commercial gain.

Where a licence is displayed above, please note the terms and conditions of the licence govern your use of this document.

When citing, please reference the published version.

Take down policy

While the University of Birmingham exercises care and attention in making items available there are rare occasions when an item has been uploaded in error or has been deemed to be commercially or otherwise sensitive.

If you believe that this is the case for this document, please contact UBIRA@lists.bham.ac.uk providing details and we will remove access to the work immediately and investigate.

Characteristics of Combustion and Emissions of 2-Methylfuran Compared to 2,5-Dimethylfuran, Gasoline and Ethanol in a DISI Engine

Chongming Wang^a, Hongming Xu^{a,b,}, Ritchie Daniel^a, Akbar Ghafourian^a,*

Jose Martin Herreros^c, Shijin Shuai^b, Xiao Ma^a

- a. University of Birmingham, Birmingham, B15 2TT, UK
- b. State Key Laboratory of Automotive Safety and Energy, Tsinghua University, Beijing
- c. E.T.S. Ingenieros Industriales, University of Castilla-La Mancha, Ciudad Real, Spain.

Abstract: Although 2,5-dimethylfuran (DMF) has been considered as a new bio-fuel candidate for spark ignition (SI) engines, since the discovery of improved methods of its production, 2-Methylfuran (MF) which is another main product of the process of dehydration and hydrogenolysis of fructose, has also been brought into the sight of fuel researchers. The energy density of MF is comparable to DMF and gasoline however very little is known about its combustion behaviors especially in automotive applications. This paper examines the results of a single cylinder spray guided direct-injection spark-ignition (DISI) engine fuelled with MF, compared to gasoline, ethanol and DMF. The regulated emissions (CO, NO_x and HC) and particulate matter (PM) as well as the unregulated emissions (formaldehyde and acetaldehyde) were measured and studied. The experiments were conducted at stoichiometric air-fuel ratio with the engine speed of 1500 rpm and loads between 3.5 and 8.5 bar IMEP using the fuel-specific optimum spark timings (MBT). The test results show that the knock suppression ability of MF is similar to DMF and superior to gasoline. Although MF has a similar chemical structure to DMF, its combustion characteristics are significantly different. Within the tested load range, MF gives rise to consistent higher indicated thermal efficiency by some 3% compared to gasoline and DMF. This increase is attributed to the fast burning rate and notable better knock

* To whom correspondence should be addressed. Email: h.m.xu@bham.ac.uk

suppression ability. MF has resulted in approximately 30% lower volumetric indicated specific fuel consumption compared with ethanol. The overall regulated emissions from MF are comparable to the other tested fuels, whereas the aldehyde emission is much lower than gasoline and bio-ethanol.

Keywords: DISI Engine; Bio-fuel; 2-Methylfuran; 2,5-Dimethylfuran; Formaldehyde; Acetaldehyde; Emissions

1. INTRODUCTION

In recent decades, greater emphasis has been made to improve the fuel economy and reduce the tailpipe emissions from vehicles due to the concerns of energy supply and global warming. Sustained research and development have been performed with bio-fuels, such as bio-ethanol [1-4] which is the most commonly used bio-fuel in SI engines due to its renewable nature and high octane number. Apart from SI engines, bio-ethanol is also used in diesel engines. Researchers from University of Minnesota have reported the application of hydrogen assisted combustion of ethanol in diesel engines [5]. Investigations on the use of diesel-ethanol in diesel engines are also available [6, 7]. However, bio-ethanol has several limitations: low energy density, high volatility and high energy consumption in production phase. Therefore, the search for superior alternatives to bio-ethanol is an important area of energy development.

Improved MF production methods were discovered in 2009. Dumesic and Román, and Zhao et al. have independently discovered and further developed a highly efficient approach of converting fructose into MF, shown in Fig.1 [8-10] as reported by *Nature* and *Science* respectively. Selective oxygen removal can be accomplished in two steps: first, by removing three oxygen atoms through dehydration to produce 5-hydroxymethylfurfural (HMF); and second, by removing two oxygen atoms through hydrogenolysis to produce MF [11, 12]. Fructose is abundant and renewable. Therefore, MF produced by this method is considered as a renewable fuel. In this process, DMF is also produced.

The author's group was the first group that has researched DMF as an engine fuel [13, 14]. They also studied the dual-injection strategy using DMF and gasoline [15] and a chapter in a book on DMF as a new bio-fuel candidate has been published [12]. The results indicate that DMF has similar combustion characteristics and emissions to gasoline, which makes it easily adoptable to current DISI technologies. Researches on this chemical by other groups are reported in other publications [16-20].

The properties of MF are similar to DMF, as shown in Table 1; some properties are more attractive as an engine fuel. The initial boiling point of MF (63°C) is much closer to gasoline (32.8°C) than DMF (92°C). Its density (913.2 kg/m³ at 20°C) is higher than DMF (889.72 kg/m³ at 20°C) and its flash point (-22°C) is lower than DMF (16°C), which would also overcome the cold engine start problems usually associated with bio-ethanol. Finally, its latent heat of vaporization (358.4 kJ/kg) is higher than DMF (330.5 kJ/kg), which would result in a higher power output in DI engines at wide open throttle in a DISI engine.

Currently, little is known about the combustion and emissions of MF. The first report [21] found that MF is more robust to cold engine starts than ethanol due to higher rates of vaporization and higher combustion stabilities. The knock suppression ability of MF was shown to be superior to gasoline, which would support the use of higher compression ratio SI engines in the drive for greater efficiencies through engine 'downsizing'. The HC emissions from MF are at least 61% lower than gasoline. However, due to the high adiabatic flame temperature of MF, the NO_x emission level is a concern.

In the present study, the combustion and emissions of MF in a single cylinder spray guided DISI engine are examined. The experiments were conducted at stoichiometric air-fuel ratio with the engine speed of 1500 rpm and loads between 3.5 and 8.5 bar IMEP using the fuel-specific optimum spark timings (MBT). The results are compared with using gasoline, ethanol and DMF. Not only the regulated emissions (CO, NO_x and HC) but also particulate matter (PM) size and number distributions and the unregulated emissions of formaldehyde and acetaldehyde were measured and studied. Fuel-specific MBT timings are used to investigate the maximized combustion performance for each fuel.

2. EXPERIMENTAL SYSTEMS AND METHODS

2.1. ENGINE AND INSTRUMENTATION

The experiments were performed on a single cylinder, spray guided, 4-stroke DISI research engine shown in Figure 2 and the engine specification is given in Table 2. The engine was coupled to a direct current (DC) dynamometer to maintain a constant speed of 1500rpm (± 1 rpm) regardless of the engine torque output. The in-cylinder pressure was measured using a Kistler 6041A water-cooled pressure transducer. All temperatures were measured with K-type thermocouples. Coolant and oil temperatures were precisely maintained at 358 K and 368 K (± 3 K) respectively, using a Proportional Integral Differential (PID) controller and heat exchangers. A 100L intake buffer tank (approximately 200 times the engine's swept volume) was used to stabilize the intake air flow.

The engine was controlled using in-house control software written in LabVIEW. The gaseous emissions were measured using a Horiba MEXA-7100DEGR gas analyzer. The accuracy for HC, NO_x and CO measurements is 1 ppm. Particulate matter (PM) emissions were measured using a Scanning Mobility Particle Sizer Spectrometer (SMPS3936) manufactured by TSI. Exhaust samples were taken 0.3 m downstream of the exhaust valve and pumped via a heated line (maintained at 464 K) to the analyzer.

2.2. TEST FUELS

The properties of the four studied fuels are listed in Table 1. Both gasoline and ethanol were supplied by Shell Global Solutions, UK. A high octane gasoline was chosen as it represents the most competitive characteristics offered by the market. The DMF was supplied by Beijing LYS Chemicals Co. Ltd. from China at 99% purity. MF was provided by Fisher Scientific, UK, with 99% purity.

2.3. EXPERIMENTAL PROCEDURE

2.3.1. ENGINE SETUP

The engine was firstly warmed up with the coolant and lubricating temperatures stabilized. All the tests were carried out at ambient air intake conditions ($298\pm 1\text{K}$), at the engine speed of 1500 rpm and stoichiometric air-fuel ratio (AFR). For each test, the pressure data from 300 consecutive cycles were recorded and then averaged.

All the tests for each fuel carried out in this work were done under the fuel-specific optimum spark timings, known as the maximum brake torque (MBT) timings. Spark sweeps were performed for each fuel at various loads (3.5-8.5 bar IMEP at 1 bar IMEP intervals). The definition used for the MBT timing was the spark timing which provides the maximum IMEP for a fixed throttle position. In the event of spark knock or combustion instability ($\text{COV of IMEP} > 5\%$), the MBT timing was retarded by 2 CAD. In such cases, the optimum ignition timing is referred as the knock-limited spark advance (KLSA).

2.3.2. QUANTIFICATION OF FORMALDEHYDE AND ACETALDEHYDE

In this investigation, the emissions of formaldehyde and acetaldehyde were investigated through the wet chemistry analysis of acidified 2,4-dinitrophenylhydrazine (DNPH) solution using HPLC. There are 13 different carbonyls being measured in CARB Method 1004 [22], however only formaldehyde and acetaldehyde are presented in this work because formaldehyde and acetaldehyde dominate carbonyls emissions in exhaust gas, the concentration of rest individual carbonyl ($\text{C} > 3$) is below 5ppm. The exhaust gas is bubbled at a constant flow rate (1 L/min) for a fixed time period (20 mins) in acidified DNPH reagent (20 ml) as supplied by Sigma Aldrich. The interaction of the carbonyls with the DNPH reagent produces DNPH-carbonyl derivatives, which can then be analyzed through reverse phase HPLC. Each test was repeated three times in order to quantify the magnitude of repeatability.

A standard solution containing formaldehyde and acetaldehyde in acetonitrile (supplied by Sigma Aldrich) was used in the calibration. The peak area of each compound in the sample was then compared to that of the calibration in order to determine its concentration.

3. RESULTS AND DISCUSSION

3.1. SPARK TIMING

The fuel-specific optimized spark timings or MBT/KLSA timings at the various loads are shown in Fig.3 (a). At 3.5 bar IMEP, there is no difference in the MBT/KLSA locations for all fuels. However, as the load increases from 4.5 bar IMEP, the MBT/KLSA locations for all the fuels start to differ. MF has similar MBT/KLSA locations with DMF within the entire load range. Ethanol allows the most advanced spark timing while the MBT/KLSA for gasoline is the most retarded. At the highest load (8.5 bar IMEP), the MBT/KLSA timing for MF is 6 CAD more advanced than gasoline. The maximum difference between MF and ethanol is 5 CAD at the highest load. Within the entire load range, the knock phenomenon can be observed when using MF, as well as DMF and gasoline. For MF and DMF knock starts to occur at 6.5 bar IMEP whereas for gasoline this is limited to 5.5 bar IMEP. No knock is observed when using ethanol.

The knock suppression ability of each fuel is related to their octane number which partially depends on the chemical structure. MF (C_5H_6O) is similar to DMF (C_6H_8O) in terms of chemical structure; the only exception is MF has one less methyl on its cyclohexene ring. The molecule of MF is relatively simple and compact whilst gasoline is a mixture of C2-C14 hydrocarbons. Overall, the chain of gasoline is the longest and the most complicated among the four studied fuels. Ethanol has the simplest and the most compact structure, of which its carbon atom number is only two. As the hydrocarbon chain length increases, the fuel becomes easier to break down when exposed to high temperatures, which increases the tendency to knock when used in a SI engine. This can be one of the reasons why MF (compact structure), unlike gasoline (long chain), has greater knock resistance.

The combustion temperature history is another important factor affecting the knock suppression ability of the fuel. This can also be influenced by the evaporative cooling effect following DI fuel supply. During the vaporization process, liquid fuel absorbs heat from ambient air, which lowers the in-cylinder air temperature. The ratios of heat of vaporization (HV) and lower heating value (LHV) used

to evaluate the cooling effect between fuels are shown in Fig.3 (b). The HV/LHV represents the amount of heat needed to evaporate the liquid fuel for one unit of fuel energy input. MF has a higher cooling effect compared to DMF and gasoline. This means that more energy is absorbed from the vaporization process by the in-cylinder charge, which helps to lower the temperature on ignition and hence discourage end-gas auto-ignition [14]. The significant HV/LHV for bio-ethanol (compared to MF) is the main reason for its high knock suppression ability.

3.2. MASS FRACTION BURNED, CID AND CD

The mass fraction burned (MFB) curve for the four tested fuels at 3.5 and 8.5 bar IMEP have been presented in Fig. 4(a) and Fig. 4(b) respectively. In-cylinder pressure data and corresponding cylinder volume data were used to calculate heat release rate against crank angle. The definition of MFB is the accumulated released heat in successive crank angle ranging from the start to the end of combustion divided by the total released heat in the whole combustion process [23]. The burning rate of MF is the fastest at both 3.5 and 8.5 bar IMEP. The difference between bio-ethanol and MF in burning rate is narrowed as load increased from 3.5 to 8.5 bar IMEP however between gasoline and MF the difference is enlarged.

The combustion initiation duration (CID), defined as the CAD interval between the start of spark discharge and 5% MFB, is presented in Fig.4 (c). The CID of MF is consistently the shortest within the entire load range. The difference between MF and gasoline in CID decreases as load increases, with a maximum of 3 CAD at 3.5 bar IMEP and a minimum of 2 CAD at 8.5 bar IMEP. This is due to an increased difference in spark timing between MF and gasoline as the load increases. As previously mentioned, at 3.5 bar IMEP, spark timing for MF and gasoline is the same whilst in 8.5 bar IMEP the spark time for MF is 6 CAD more advanced. Advanced spark timing prolongs the CID due to the lower in-cylinder temperature and pressure at the instance of spark discharge. Due to ethanol's significant cooling effect and the advanced spark timing at high load, the difference in CID between MF and

ethanol is increased from 1 CAD at 3.5 bar IMEP to 2 CAD at 8.5 bar IMEP. Between MF and DMF, their difference in CID maintains the same (2 CAD) throughout the entire load range.

The combustion duration (defined by 10%-90% MFB interval in CAD) at various loads for each fuel is shown in Fig.4 (d). As presented, MF consistently has the shortest CD within the entire load range, whilst gasoline the longest. Unlike the difference in CID, the difference in CD between MF and gasoline increases with load. The maximum difference between MF and gasoline (7 CAD) can be seen at 8.5 bar IMEP and the minimum difference (4 CAD) is at 3.5 bar IMEP. The CD for MF at 8.5 bar IMEP is about 3 and 2 CAD shorter than ethanol and DMF, respectively.

The faster burning rate of oxygenized hydrocarbon has already reported by many publications [24-26]. This can also be used to explain why MF, like DMF and ethanol, has a shorter CD compared with gasoline (no oxygen element in its molecule). The benefit of shorter CID and CD for MF is higher combustion stability as shown in Fig.5. The coefficient of variations (COV) of IMEP for MF is consistently lower than other three studied fuels. Higher combustion stability indicates that MF has an advantage when used in lean burn or deep stratified combustion modes. The chance of misfire is minimized and unburned HCs dramatically lowered.

3.3. IN-CYLINDER PRESSURE AND TEMPERATURE

The in-cylinder pressure for four tested fuels at 3.5 and 8.5 bar IMEP have been presented in Fig. 6(a) and Fig. 6(b) respectively. At 3.5 bar IMEP, MF has much highest in-cylinder pressure between 10-20 CAD. At 8.5 bar IMEP, the in-cylinder pressure for MF and bio-ethanol almost matches and both are higher than DMF and gasoline.

The maximum in-cylinder pressure at various loads for each fuel is shown in Fig.6 (c). MF consistently produces the highest in-cylinder peak pressure within the entire load range. Its maximum in-cylinder pressure does not peak at 8.5 bar IMEP. As expected, gasoline has the lowest peak pressure among the four fuels, which peaks near 7.5 bar IMEP. The difference between MF and gasoline in peak

pressure increases as load increases, with 4 and 15 bar difference at 3.5 and 8.5 bar IMEP, respectively. Even though MF has higher peak pressure than ethanol, their differences decrease as load increases. At 3.5 bar IMEP, the peak pressure for MF is 2.8 bar higher than ethanol. However, at 8.5 bar IMEP, their peak pressures are nearly the same. As to MF and DMF, their peak pressure differences keep almost constant within the entire load range, which is consistent with their constant differences in combustion duration.

There are two major factors that attribute to the significant high peak pressure for MF: advanced spark timing and short combustion duration. Shorter combustion duration for MF leads to more accumulated energy released around top dead centre (TDC), which has significantly positive effect on its peak in-cylinder pressure. MF has the same spark timing with DMF within the entire load range. However due to its shorter combustion duration, its peak pressure is consistently higher than DMF. The combination of advanced spark timing and shorter combustion duration makes MF to generate much higher peak pressure than gasoline.

The theoretical maximum in-cylinder temperature shown in Fig.6 (d) is calculated using a detailed engine gas-dynamics and thermodynamics model firstly described in [13], where the match of experimental and simulated IMEP and maximum pressure is remarkably good. Some fundamental assumptions are made according to the book by Heywood [23]. The model does not include detailed chemical kinetics because the reaction mechanisms are very complex. Instead, the ideal gas law is used and combined with the prediction of trapped residuals and fuel vaporization behavior to estimate the in-cylinder gas temperature. The results represent the global averaged gas temperatures for MF, DMF, bio-ethanol and gasoline. When simulating the combustion of gasoline, the fluid properties of indolene were used. The known fuel properties of MF and DMF were inputted but some unknown properties, such as the viscosity-temperature behavior, were taken from indolene. The SI Wiebe combustion sub-model was also used and this required the input of CA50 and CAD10-90, in order to match in-cylinder

peak temperature and IMEP to within 99.5%. The model was validated using known combustion performance data to maintain the volumetric efficiencies (VE) to within 5% at all tested engine loads.

As load increases peak temperature increases for each fuel. MF generates the highest peak temperature whilst ethanol the lowest. Peak temperature, like peak pressure, is highly dependent on spark timing and combustion duration. The trend of peak temperature and peak pressure in MF as well as DMF and gasoline is consistent. Although MF case has the same spark timing with DMF, the shorter combustion duration of MF makes its peak temperature higher than DMF. As burning rate increases, heat release rate during combustion process increases, which contributes to generate higher peak temperature. The MF case has significant higher peak temperature than ethanol. This is due to not only shorter combustion duration of MF, but also the ethanol's significant cooling effect which lowers its initial combustion temperature as well as combustion temperature.

3.4. INDICATED THERMAL EFFICIENCY

The indicated thermal efficiencies (including pumping loss) at various loads for each fuel are shown in Fig.7. The performance of MF is better than gasoline and DMF during the entire load range. At 8.5bar IMEP, the indicated thermal efficiency for MF is 1.4% and 2.7% higher compared to DMF and gasoline, respectively. The indicated thermal efficiency for MF peaks around 7.5-8.5bar IMEP whilst gasoline peaks around 6.5-7.5bar IMEP.

Heat transfer loss is one important negative factor on indicated thermal efficiency. Higher combustion temperature encourages more heat transfer loss to the cylinder wall. The significant high combustion temperature (indicated by peak in-cylinder pressure) of MF is one main reason that its net indicated thermal efficiency is lower than that of ethanol.

3.5. COMBUSTION EFFICIENCY

The combustion efficiency is presented in Fig.8 to describe the completeness of combustion. In spark ignition engine running under stoichiometric air-fuel ratio, the combustion efficiency is between 92-98% [23]. The incomplete combustion is due to the unreleased chemical energy contained in incompletely combusted products, such as CO, H₂, and unburned hydrocarbons. In this paper, the expression used to calculate the combustion efficiency is as follows [23]:

$$\text{Combustion Efficiency: } \eta_c = 1 - \frac{\sum x_i * Q_{LHV_i}}{[\dot{m}_{fuel}/(\dot{m}_{air} + \dot{m}_{fuel})] * Q_{LHV_{fuel}}} \quad (1)$$

where x_i and Q_{LHV_i} represent the mass fractions and lower heating values (LHV) of HC, CO, nitric oxide (NO) and hydrogen (H₂), respectively.

It is clear that MF has higher combustion efficiency (96%) than DMF (95.7%) and gasoline (95.3%) whilst ethanol (96.7%-97.5%) the highest. Combustion efficiency is closely related with combustion temperature, which can be referenced by peak in-cylinder temperature (Fig.6 (b)). Higher combustion temperature contributes to more complete combustion and HC post-oxidization during exhaust stroke. This principle works with MF, gasoline, and DMF. Relative oxygen content in each fuel also another important factor affects the level of combustion completeness. Higher oxygen element in fuel molecule encourages the availability of oxygen during combustion, which helps to increase combustion efficiency. Amongst the four fuels, the oxygen content in MF (O/C=0.2) is lower than ethanol (O/C=0.5), which can explain that ethanol has advantages over MF in terms of combustion efficiency.

3.6. INDICATED SPECIFIC FUEL CONSUMPTION

The gravimetric indicated specific fuel consumptions (GisFC) for each fuel are shown in Fig.9 (a). Within the entire load range, MF has about 12%-13% lower GisFC than ethanol due to its higher energy density. Even though MF has 5.4% lower energy density (LHV in mass) than DMF, its relatively higher indicated thermal efficiency makes its GisFC much closer (2.6%-3.7% higher) to

DMF. Due to the relatively higher energy density of gasoline, MF has disadvantage compared with gasoline on GisFC. The dash line in Fig.9 (a) shows the gasoline GisFC for MF which is converted from the measurement of MF fueling rate to corresponding gasoline fueling rate for the same energy content [11]. It can be seen that MF is superior to gasoline in this sense as indicated by its higher indicated thermal efficiency. The volumetric indicated specific fuel consumption (VisFC) is illustrated in Fig.9 (b). MF is close to gasoline and DMF, and much less (30% less at 3.5 bar IMEP) than ethanol in terms of VisFC.

3.7. GASEOUS EMISSIONS

The regulated emissions (NO_x , HC, and CO) are presented in Fig.10. The formation of NO_x is exponentially dependant on the combustion flame temperature [23]. This trend is observed in Fig.10 (a) and Fig.6 (b) (in-cylinder peak temperature). MF produces the highest NO_x emissions due to its significant in-cylinder peak temperature. The maximum difference in NO_x emissions between MF and other three fuels is at the lower load end 3.5 bar IMEP, where MF generates 82%, 281% and 40% more NO_x emissions than gasoline, ethanol and DMF, respectively. For each fuel, the NO_x increases with load, and a similar peak in-cylinder temperature trend with the load can also be seen in Fig.6 (b). It has been reported that the relative NO_x emissions can be related to fuel property, the H/C ratio [14, 27]. Fuel with higher H/C ratio indicates lower NO_x emissions. For the present data, this principle applies.

The indicated specific hydrocarbon (HC) emissions for each fuel are shown in Fig. 10 (b). It is distinct that MF has significant advantage on HC emissions over gasoline and DMF. The HC emissions for MF have inverse relationship with load, which also can be seen for gasoline and DMF. This is mainly due to the increased in-cylinder temperature with load. Higher temperature makes HC post-oxidization much easier to take place. This trend is verified by the inverse relationship between the in-cylinder peak temperature and HC emission for MF, DMF and gasoline.

Additionally, one more principle applies that the fuel with more oxygen element in their molecule tends to produce lower HC emissions. Higher oxygen element in MF leads to lower HC emissions for

gasoline and DMF. However, the advantage of MF over gasoline and DMF in terms of HC emission (measured by Horiba using FID detector) could be subjected to reduced sensitivity of FID to oxygenated hydrocarbon, reported by Wallner [28] and Price et al [29].

The indicated specific carbon monoxide emissions (isCO) for each fuel at various loads are shown in Fig.10(c). Generally, MF has higher CO emissions than gasoline and ethanol. CO emissions are highly dependent on the fuel/air equivalence ratio, which dramatically increases as air fuel mixture becomes rich. Even though all the tests are carried out with stoichiometric air fuel ratio, the homogenous level for each fuel in the DI combustion chamber differs due to their spray characteristics and volatility property; shorter spray penetration leads to lower chance of piston and cylinder wall wetting. Liquid fuel film on cylinder wall or piston top has difficulty to be fully evaporated. Lower volatility can also deteriorate the homogenous level. Gasoline has advantages over MF in CO emissions. This is because gasoline is relatively easier to form combustible mixture due to its significant volatility property. Additionally, its high energy density leads to shorter injection time and shorter the fuel spray penetration. All these tend to reduce spray impingement on the piston crown. This fact can be used to explain why gasoline has the lowest CO emission level in most conditions. On the other hand, ethanol fuel molecule is highly oxygenated; hence more oxygen is available for completed combustion [30], which contributes to offsetting the disadvantage caused by the piston wetting. The overall effect is that ethanol has lower CO emissions compared with DMF and MF.

The acetaldehyde (CH_3CHO) and formaldehyde (CH_2O) emissions for MF at a selected engine upper-medium load condition (6.5bar IMEP) are presented in Fig. 11. The formaldehyde emission from MF is 32.7ppm, which is much lower than gasoline (179.4ppm), ethanol (155.7ppm), and DMF (68.4ppm). The acetaldehyde emission from MF at the same load is 32.3ppm, which is comparable to DMF (26.1ppm) and methanol (26.3ppm), lower than gasoline (53.9ppm), and significantly lower than ethanol (303.1ppm).

3.8. PM EMISSIONS

Typically, the PM size distribution consists of two modes [31]: the nucleation mode which usually has more influence in number of particles and the accumulation mode which determines the particle mass distribution due to its higher size. Fig.12 (a) shows the raw PM size distributions for MF and gasoline at 6.5bar IMEP. For both MF and gasoline, there are overlaps between nucleation mode and accumulation mode. Many researchers have used diameter range to separate nucleation and accumulation mode. Kittelson suggested: nucleation mode (<50 nm), accumulation mode (50-1000 nm) [32]. Eastwood suggested: nucleation mode (<100 nm), accumulation mode (100-900 nm) [31]. In this study, two modes are separated using a Matlab script developed by University of Castilla-La Mancha [33], which is shown in Fig.12 (b). The notations N, A and T mean nucleation mode, accumulation mode and total PM emission distribution, respectively. A summary of PM emissions is listed in Table 3. MF has much smaller mean diameter (21.6nm) in nucleation mode than that of gasoline (41.7nm). As to the mean diameter of accumulation mode, there is no apparent difference between those two fuels. MF has 57.9% less number in nucleation mode and 238.3% less mass in accumulation mode compared with gasoline. For MF, nucleation mode accounts for 97.1% and 19.5% in total number and total mass respectively. For gasoline, those two figures are 92.2% and 25.5% respectively. The fuel properties have direct impact on the PM emissions. High oxygenated fuels, like MF (O/C=0.2), tend to produce less soot.

The soot level can dramatically affect the shape of the particle size distribution. Higher soot emissions increase the chance of gaseous HC adsorption and condensation on its surface forming wet coating, reducing the available hydrocarbons for nucleation. Hydrocarbons are adsorbed or condensed on soot particles, which increase the size and increase the chance for wet soot to collide with each other and form even bigger soot particles. Higher gaseous HC emissions tend to increase the total number of particles and increase the mean diameter for both nucleation and accumulation mode. From Fig.10 (b), it is clear that at 6.5bar IMEP, MF has the much lower HC emissions (3.63g/kWh) than that of gasoline (5.98g/kWh). The higher oxygen content in MF molecule and lower HC emissions compared with that

of gasoline can be used to explain why MF has smaller mean diameter and lower number in nucleation mode of PM emissions.

4. CONCLUSIONS

This paper examines the combustion performance and emissions of MF used in a single cylinder spray guided DISI engine for the load condition of 3.5 to 8.5 bar IMEP at the engine speed of 1500 rpm and stoichiometric air/fuel ratio. The results are compared with gasoline, ethanol and another promising bio-fuel candidate, DMF. Based on the experimental results and analysis, the following conclusions can be drawn:

1. Although MF has a similar chemical structure to DMF, its combustion characteristics are notably different. MF has a much faster burning rate, which makes its CID and combustion duration the shortest among the four studied fuels at equivalent engine conditions. At the higher load end tested 8.5 bar IMEP, the combustion duration for MF is about 7, 3 and 2 CAD shorter than gasoline, ethanol and DMF, respectively. Its fast burning rate also makes MF generate the highest in-cylinder peak pressure, which is even higher than for ethanol.
2. Similar to DMF, MF has better knock suppression ability than gasoline. This is due to its simpler and more compact molecule structure and also faster burning rate. This makes MF a competitive fuel to be used in higher compression ratio SI engines.
3. Due to the combined effect of significant knock suppression abilities, fast burning rate and high in-cylinder peak pressure, MF consistently produces higher indicated thermal efficiency than gasoline and DMF within the entire tested load range. At 8.5 bar IMEP, the indicated thermal efficiency for MF is increased by 1.4% and 2.7% as compared with DMF and gasoline respectively.
4. MF has the volumetric fuel consumption rate comparable with gasoline and DMF. MF has significant advantage over ethanol with a lower VisFC (as typical, by 30% at 3.5 bar IMEP)

due to its relatively high energy density and mass density, despite of its lower indicated thermal efficiency than the former.

5. At 8.5 bar IMEP, MF produces 73% and 40% less HC emissions than gasoline and DMF respectively. This is mainly because of its high combustion temperature and high oxygen content in its molecule. However, due to the high in-cylinder temperature, MF produces higher NO_x emissions. The maximum difference in NO_x emissions between MF and the other three fuels is at the lower load end tested 3.5 bar IMEP, where MF generates 82%, 281% and 40% more NO_x emissions than gasoline, ethanol and DMF, respectively.
6. The formaldehyde emission from MF at the upper-medium load 6.5bar IMEP is 32.7 ppm, which is the lowest among the four studied fuels. The acetaldehyde emission from MF at 6.5bar IMEP is 32.3 ppm, which is comparable to DMF and lower than gasoline and ethanol.
7. At 6.5bar IMEP, MF has 57.9% less PM number in nucleation mode and 238% less PM mass in accumulation mode compared with gasoline. The mean diameter in nucleation mode for MF (27.6 nm) is much smaller than that of gasoline (41.7 nm). The advantage for MF over gasoline on PM emissions is linked to its lower HC emissions and higher oxygen content in its molecule.

ACKNOWLEDGMENTS

This work was conducted in the Future Engines and Fuels Lab at the University of Birmingham and financially supported by the Engineering and Physical Sciences Research Council (EPSRC) through the Research Grant EP/F061692/1. The authors thank Peter Thornton and Carl Hingley for their technical support of the engine testing facility and Farshad Eslami for his contribution to the measurement of the calorific values of the tested fuels. The authors thank Dr Lixia Wei (Royal Society sponsored Sino-British Research Fellow) for the contribution in helping with unregulated emission results analysis.

REFERENCES

1. Kintisch E., "Energy Research: BP Bets Big on UC Berkeley for Novel Biofuels Center," Science, 315(5813): 747, 2007.
2. Atsumi S., Hanai T., Liao J.C., "Non-fermentative Pathways for Synthesis of Branched-Chain Higher Alcohols as Biofuels," Nature, 451(7174): 86—89, 2008.
3. Demirbas A., "Progress and Recent Trends in Biofuels," Pro. Energy and Combust Sci 33: p.1-18, 2007.
4. Agarwal, A.K., "Biofuels (Alcohols and Biodiesel) Applications as Fuels for Internal Combustion Engines," Pro. Energy and Combust. Sci., 33 (3), p. 233–271, 2007.
5. Rakopoulos, D.C., Papagiannakis, R.G., Kyritsis, D.C., "Combustion heat release analysis of ethanol or n-butanol diesel fuel blends in heavy-duty DI diesel engine," Fuel, 90:1855-67, 2011.
6. Bika, A.S., Franklin, L., David, B.K., Hydrogen assisted combustion of ethanol in Diesel engines, Department of Mechanical Engineering, University of Minnesota, Minneapolis MN
7. Scania, New highly efficient diesel-ethanol engine- ready to cut fossil CO₂ emissions by 90%, PRESS info, 2007
8. Zhao, H., Holladay, J.E., Brown, H. and Zhang, Z.C., "Metal Chlorides in Ionic Liquid Solvents Convert Sugars to 5-Hydroxymethylfurfural," Science 316: p.1597–600, 2007.
9. Roman-Leshkov, R., Barrett, C.J., Liu, Z.Y. and Dumesic, J.A., "Production of Dimethylfuran for Liquid Fuels from Biomass-Derived Carbohydrates," Nature 447: p. 982–986, 2010.
10. Dumesic, J.A., Roman-Leshkov, Y., and Chhedha, J.N., "Catalytic Process for Producing Furan Derivatives from Carbohydrates in a Biphasic Reactor," US: World Intellectual Property, 2007.
11. Yuriy Roman-Leshkov, Biomass-Derived Furanic Compounds for the Production of Fuels and Chemical Intermediates, Presentation, 2009.
12. Tian, G., Xu, H., Daniel, R., Biofuel Production-Recent Developments and Prospects, chapter "DMF-A New Biofuel Candidate," 2011.
13. Zhong, S., Daniel, R., Xu, H., Wyszynski, M. L., "Combustion and Emissions of 2,5-Dimethylfuran in a Direct-Injection Spark-Ignition Engine," Energy & Fuels, 24(5), p. 2891-2899, 2010.
14. Daniel, R., Tian, G., Xu, H., Wyszynski, M.L., Wu, X. and Huang, Z., "Effect of Spark Timing and Load on a DISI Engine Fuelled with 2,5-Dimethylfuran," Fuel 90: p. 449-458, 2011.
15. Wu, X., Daniel, R., Tian, G., Xu, H., Huang, Z. and Richardson, D., "Dual-Injection: the Flexible, Bi-fuel Concept for Spark-Ignition Engines fuelled with Various Gasoline and Biofuel Blends," Applied Energy 88: p. 2305-2314 , 2011.

16. Wu, X., Huang, Z., Jin, C., Wang, X., Zheng, B., Zhang, Y. and Wei, L., "*Measurements of Laminar Burning Velocities and Markstein Lengths of 2,5-Dimethylfuran Air Diluent Premixed Flames*," *Energy Fuels* 23: p. 4355–62, 2009.
17. Wu, X., Huang, Z., Yuan, T., Zhang, K. and Wei, L., "*Identification of the Combustion Intermediates in a Low-Pressure Premixed Laminar DMF/Oxygen/argon Flame with Tunable Synchrotron Photo Ionization*," *Combustion Flame* 156: p. 1365-1376, 2009.
18. Tian, G., Xu, H., Daniel, R., Li, H., Shuai, S. and Richards, P., "*Laminar Burning Velocities of DMF Compared with Ethanol and Gasoline*," *Energy & Fuels* 7: p. 3898-3905, 2010.
19. Wu, X., Li, Q., Fu, J., Huang, Z., Daniel, R., Tian, G., Xu, H., "*Laminar burning characteristics of 2-5-dimethylfuran and iso-octane blend at elevated temperatures and pressures*," *Fuel*, 95:234-240, 2012,
20. Li, Q., Fu, J., Wu, X., Tang, C., Huang, Z., "*Laminar flame speeds of DMF-iso-octane-air-N₂/CO₂ mixtures*," *Energy and Fuels*, 26(2): 917-9925, 2012,
21. Thewes, M., Muether, M., Pischinger, S., Budde, M., Brunn, A., Seher, A., Adomeit, P., klankermayer, J., "*Analysis of the Impact of 2-Methylfuran on Mixture Formation and Combustion in a Direct-Injection Spark-Ignition Engine*," *Energy & Fuels*, 25 (12), p. 5549–5561, 2011.
22. California Environmental Protection Agency, *Determination of Hazardous Air Pollutants from Vapor Recovery Processors*, 2001.
23. Heywood, J.B., *Internal Combustion Engine Fundamental*, McGraw-Hill Book Company, 1989.
24. Aleiferis, P., Malcolm, J., Todd, A., and Cairns, A., "An Optical Study of Spray Development and Combustion of Ethanol, Iso-Octane and Gasoline Blends in a DISI Engine," SAE Technical Paper 2008-01-0073, 2008.
25. Cairns, A., Stansfield, P., Fraser, N., and Blaxill, H., "A Study of Gasoline-Alcohol Blended Fuels in an Advanced Turbocharged DISI Engine," *SAE Int. J. Fuels Lubr.* 2(1):41-57, 2009.
26. Yeliana, Cooney, C., Worm, J., and Naber, J., "The Calculation of Mass Fraction Burn of Ethanol-Gasoline Blended Fuels Using Single and Two-Zone Models," SAE Technical Paper 2008-01-0320, 2008.
27. Harrington, J.A., and Shishu R.C., "*A Single-Cylinder Engine Study of the Effects of Fuel Type, Fuel Stoichiometry, and Hydrogen-to-Carbon Ratio and CO, NO, and HC Exhaust Emissions*," SAE 730476, 1973.
28. Wallner, T. and Miers, S., "*Combustion Behavior of Gasoline and Gasoline/Ethanol Blends in a Modern Direct-Injection 4-Cylinder Engine*," SAE Paper 2008-01-0077, 2008.
29. Price, P., Twiney, B., Stone, R., Kar, K., Walmsley, H., "*Particulate and Hydrocarbon Emissions from a Spray Guided Direct Injection Spark Ignition Engine with Oxygenate Fuel Blends*," SAE Paper 2007-01-0472, 2007.
30. Turnera, D., Xu, H., "*The Effect of Bio-Ethanol on Direct Injection Spark Ignition (DISI) Engine Performance*," *Fuel* 90: p. 1999–2006, 2011.

31. Eastwood P., *Particulate Emissions from Vehicles*. John Wiley & Sons. Inc., 2007.
32. Kittelson, D.B., "*Engines and Nanoparticles: A Review*," *Journal of Aerosol Science* 29 (5/6): 575-588, 1997.
33. Armas, O., Gómez, A., and Mata, C., "*Methodology for Measurement of Diesel Particle Size Distributions from A City Bus Working in Real Traffic Conditions*," *Measurement Science and Technology* 22, 105404 (11pp), 2011.
34. Janet, Y., Earl. C., and McCormick, R., "*Utilization of Renewable Oxygenates as Gasoline Blending Components*," National Renewable Energy Laboratory, 2011.

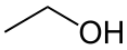
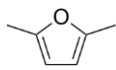
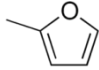
List of Tables

Table 1 Properties of the Fuels Studied

Table 2 Experimental Single Cylinder Engine Specification

Table 3 Summary of PM Emissions for MF and Gasoline at 6.5 bar IMEP

Table 1 Properties of the Fuels Studied

	Gasoline	Ethanol	DMF	2-Methylfuran
Chemical Formula	C2-C14			
H/C Ratio	1.795	3	1.333	1.2
O/C Ratio	0	0.5	0.167	0.2
Gravimetric Oxygen Content (%)	0	34.78	16.67	19.51
Density @ 20 °C (kg/m ³)	744.6	790.9*	889.7*	913.2**
Research Octane Number (RON)	96.8	107‡	101.3†	103**
Motor Octane Number (MON)	85.7	89‡	88.1†	86**
Stoichiometric Air-Fuel Ratio	14.46	8.95	10.72	10.05
LHV (MJ/kg)	42.9	26.9*	32.89*	31.2**
LHV (MJ/L)	31.9	21.3*	29.3*	28.5**
Heat of Vaporization (kJ/kg)	373	R4‡	332	358.4**
Initial Boiling Point (°C)	32.8	78.4	92	64.7

*Measured at the University of Birmingham, 2010.

**Yanowitz, J., Christensen, E., and McCormick, R., "Utilization of Renewable Oxygenates as Gasoline Blending Components," NREL/TP-5400-50791, 2011 [34].

† API Research Project 45, 1956.

‡ Heywood, J.B., Internal Combustion Engine Fundamentals, McGraw-Hill, 1989 [23].

Table 2 Experimental Single Cylinder Engine Specification

Engine Type	4-Stroke, 4-Valve
Combustion System	Dual-Injection: Spray Guided DISI
Swept Volume	565.6 cc
Bore x Stroke	90 x 88.9 mm
Compression Ratio	11.5:1
Engine Speed	1500 rpm
DI Pressure and Injection Timing*	15MPa, 280 °bTDC
Intake Valve Opening*	16.5 °bTDC
Exhaust Valve Closing*	36.7 °aTDC

*0° bTDC refers to TDC during 'valve overlap'

Table 3 Summary of PM Emissions for MF and Gasoline at 6.5 bar IMEP

	Nucleation Mode		Accumulation Mode	
	<i>ULG</i>	<i>MF</i>	<i>ULG</i>	<i>MF</i>
Mean Diameter (nm)	41.7	27.6	94.7	102.8
Number (#/cm ³)	3.71E+05	2.35E+05	31192	6903
Mass(g/cm ³)	18.51	3.86	53.99	15.96

List of Figures

- Figure 1** Paths for Converting Carbohydrates to MF (Roman-Leshkov et al, 2007)
- Figure 2** (a) Schematic of Engine and Instrumentation Setup (b) 3D Cylinder Head Diagram
- Figure 3** (a) MBT/KLSA Spark Timings at Various Engine Loads for MF, DMF, Ethanol and Gasoline and (b) Ratio of Heat of Vaporization (HV) and Low Heated Value (LHV)
- Figure 4** (a) Mass Fraction Burned at 3.5 bar IMEP (b) Mass Fraction Burned at 8.5 bar IMEP (c) Initial Combustion Duration 3.5-8.5bar IMEP (d) Combustion Duration at 3.5-8.5bar IMEP for MF, DMF, Ethanol and Gasoline
- Figure 5** COV of IMEP at Various Engine Loads for MF, DMF, Ethanol and Gasoline
- Figure 6** (a) In-Cylinder pressure at 3.5 bar IMEP (b) In-Cylinder pressure at 8.5 bar IMEP (c) Maximum In-Cylinder Pressures at 3.5-8.5 bar IMEP (d) Simulated Maximum In-Cylinder Temperature at 3.5-8.5 bar IMEP for MF, DMF, Ethanol and Gasoline
- Figure 7** Indicated Thermal Efficiency at Various Engine Loads for MF, DMF, Ethanol and Gasoline
- Figure 8** Combustion Efficiency for MF, DMF, Ethanol and Gasoline at Various Engine Loads
- Figure 9** Indicated Specific Fuel Consumption at Various Engine Loads for MF, DMF, Ethanol and Gasoline
- Figure 10** Indicated Specific Gaseous Emissions at Various Engine Loads for MF, DMF, Ethanol and Gasoline
- Figure 11** (a) Acetaldehyde and (b) Formaldehyde Emissions for MF, DMF, Ethanol and Gasoline at 6.5bar IMEP

Figure 12 (a) Total PM Size Distributions (b) Separation of Nucleation and Accumulation Mode
for MF and Gasoline at 6.5 bar IMEP

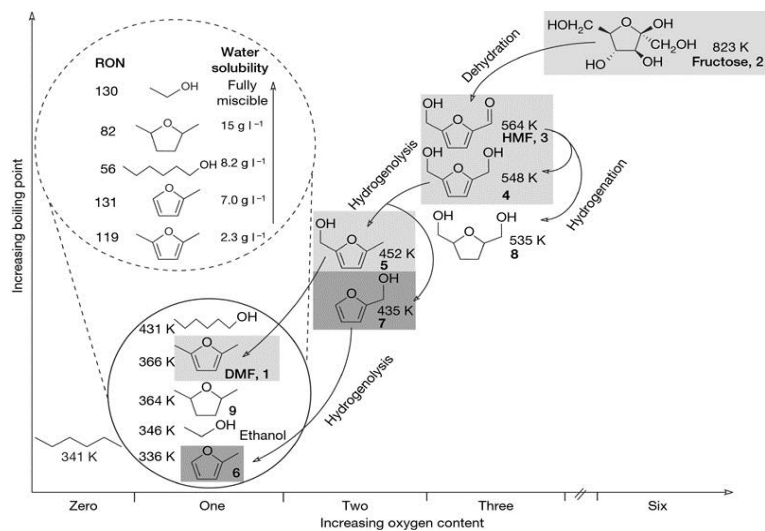


Figure 1 Paths of Converting Carbohydrates to MF (Roman-Leshkov et al, 2007)

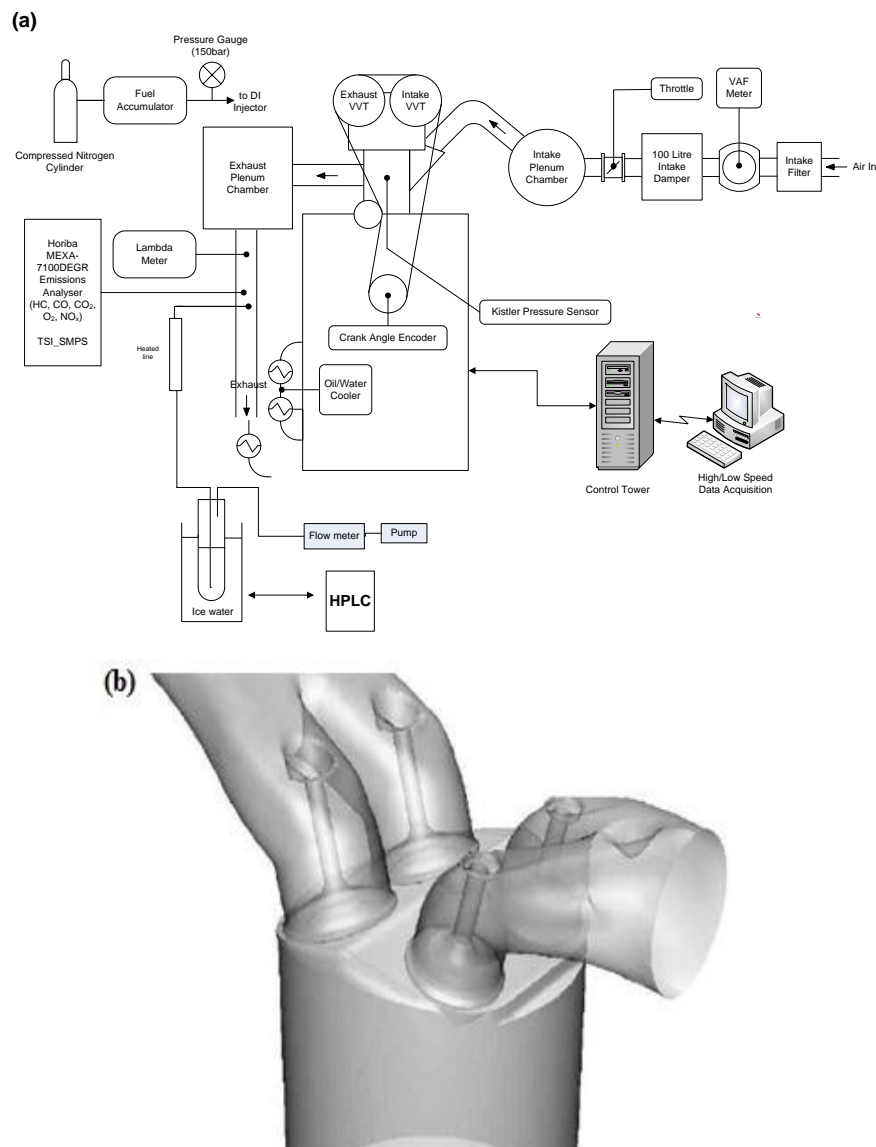


Figure 2 (a) Schematic of Engine and Instrumentation Setup (b) 3D Cylinder Head Diagram

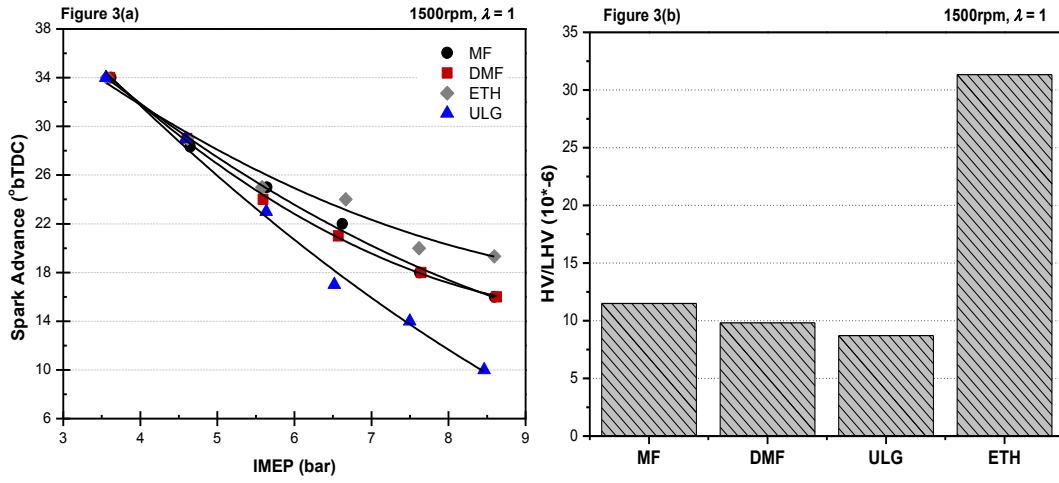


Figure 3 (a) MBT/KLSA Spark Timings at Various Engine Loads for MF, DMF, Ethanol and Gasoline and (b) Ratio of Heat of Vaporization (HV) and Low Heated Value (LHV)

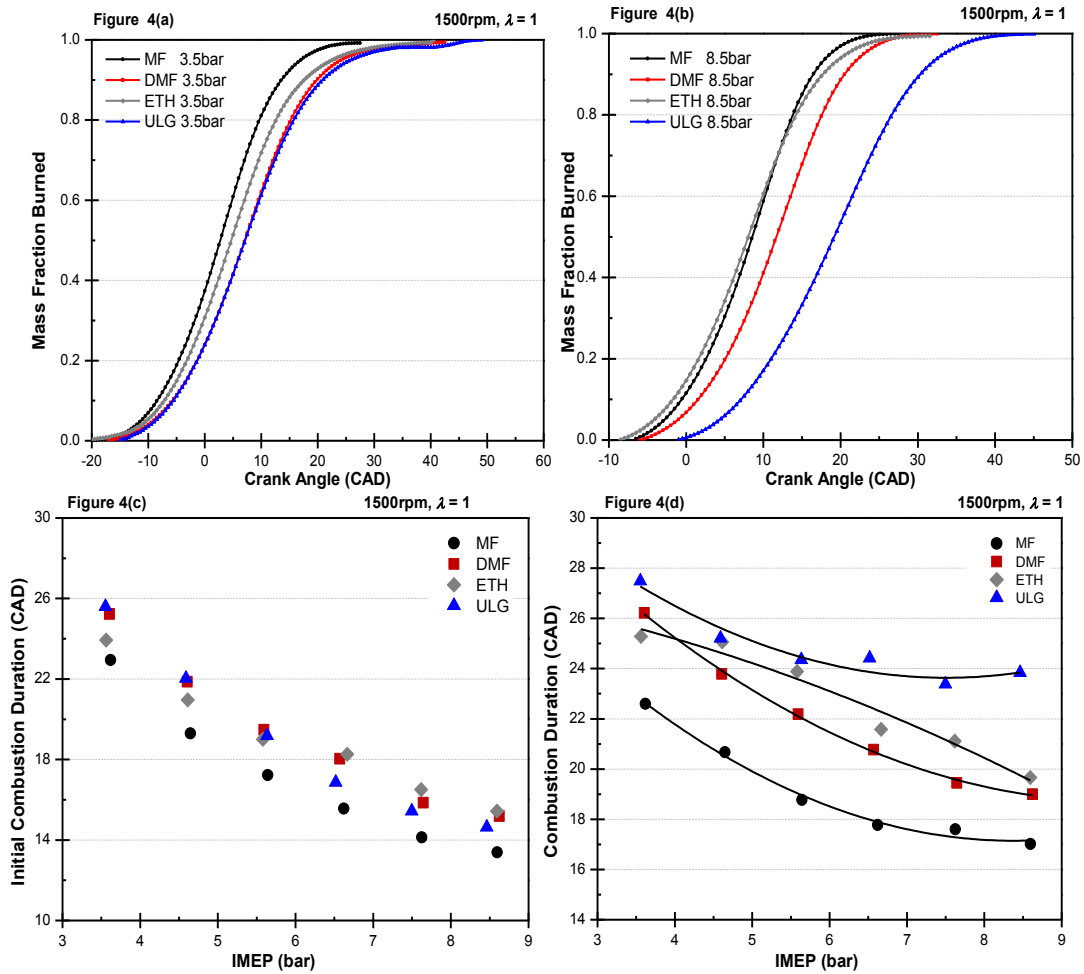


Figure 4 (a) Mass Fraction Burned at 3.5 bar IMEP (b) Mass Fraction Burned at 8.5 bar IMEP (c) Initial Combustion Duration 3.5-8.5bar IMEP (d) Combustion Duration at 3.5-8.5bar IMEP for MF, DMF, Ethanol and Gasoline

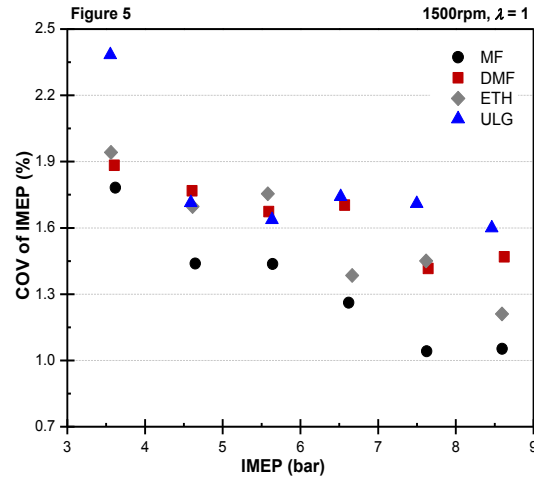


Figure 5 COV of IMEP at Various Engine Loads for MF, DMF, Ethanol and Gasoline

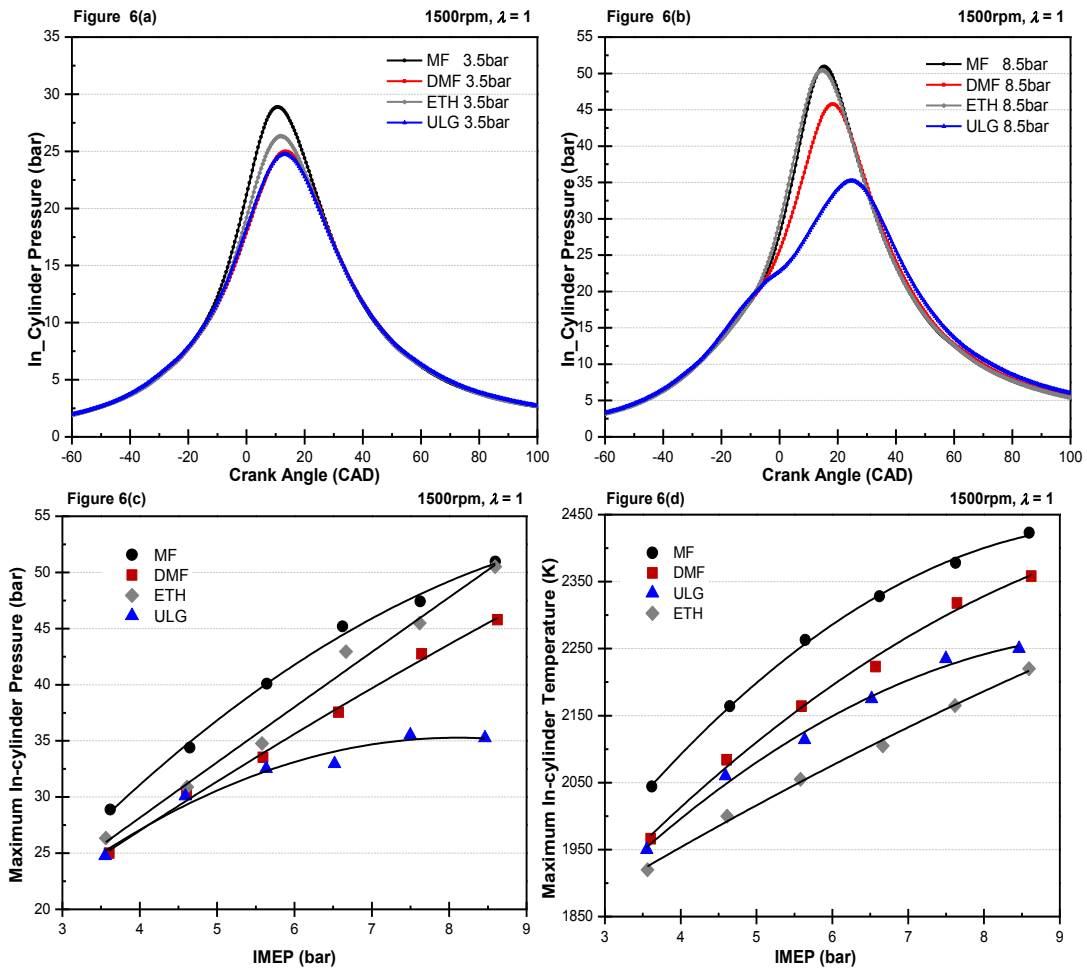


Figure 6 (a) In-Cylinder pressure at 3.5 bar IMEP (b) In-Cylinder pressure at 8.5 bar IMEP (c) Maximum In-Cylinder Pressures at 3.5-8.5 bar IMEP (d) Simulated Maximum In-Cylinder Temperature at 3.5-8.5 bar IMEP for MF, DMF, Ethanol and Gasoline

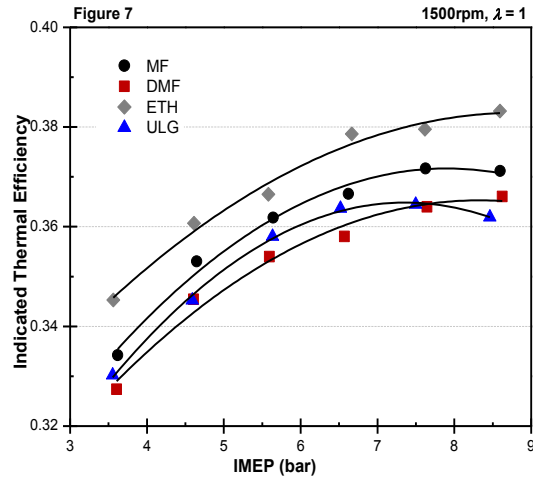


Figure 7 Indicated Thermal Efficiency at Various Engine Loads for MF, DMF, Ethanol and Gasoline

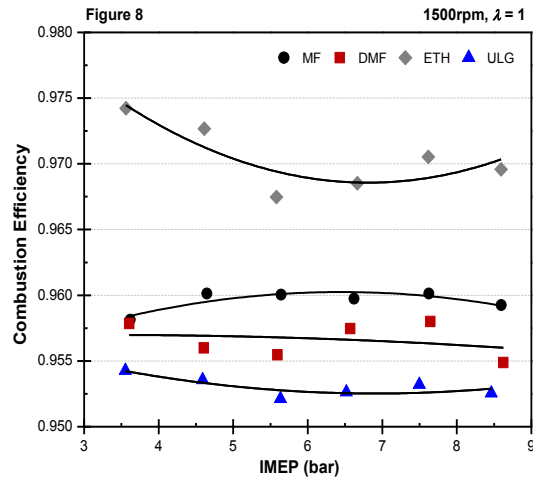


Figure 8 Combustion Efficiency for MF, DMF, Ethanol and Gasoline at Various Engine Loads

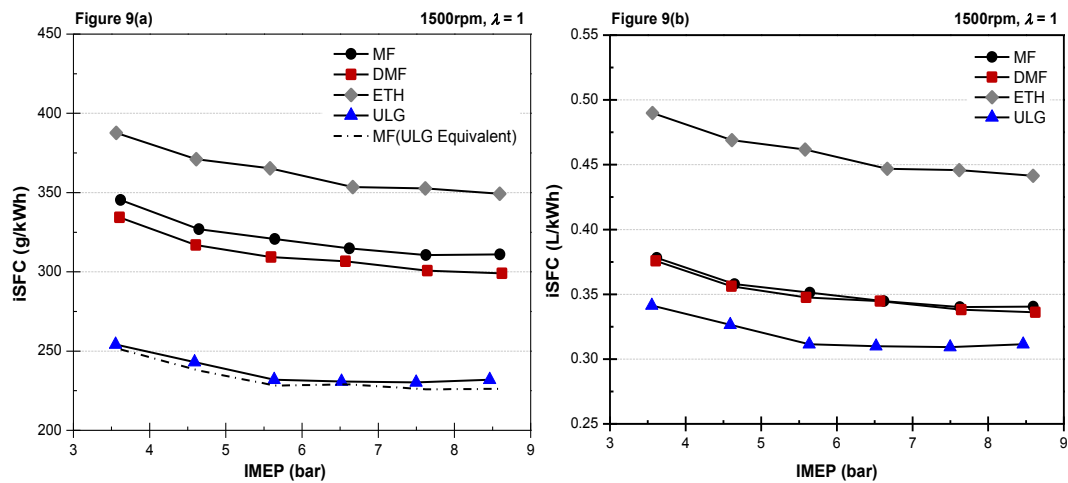


Figure 9 Indicated Specific Fuel Consumption at Various Engine Loads for MF, DMF, Ethanol and Gasoline

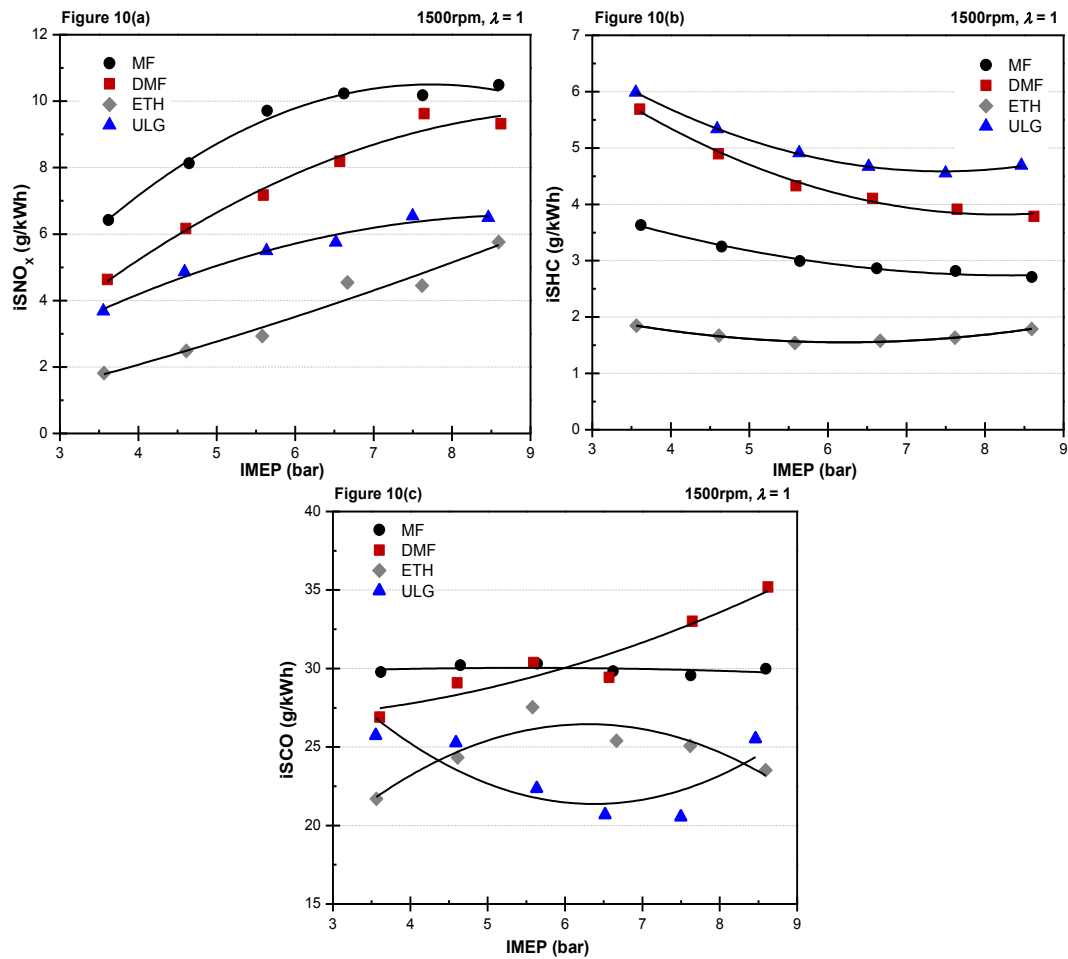


Figure 10 Indicated Specific Gaseous Emissions at Various Engine Loads for MF, DMF, Ethanol and Gasoline

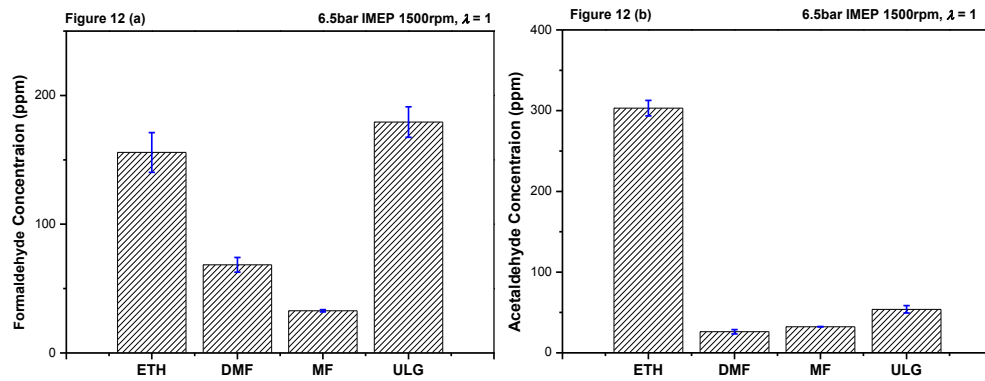


Figure 11 (a) Acetaldehyde and (b) Formaldehyde Emissions for MF, DMF, Ethanol and Gasoline at 6.5bar IMEP

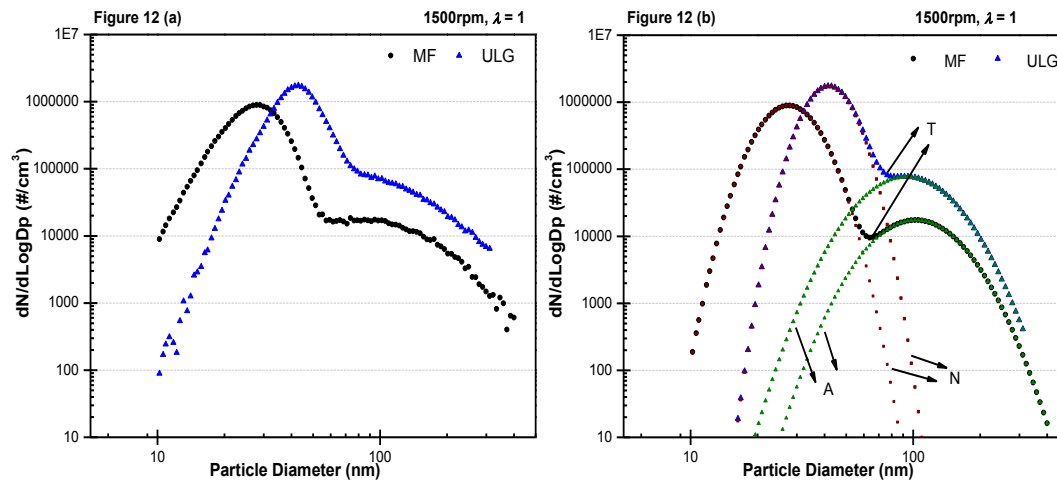


Figure 12 (a) Total PM Size Distributions (b) Separation of Nucleation and Accumulation Mode for MF and Gasoline at 6.5 bar IMEP

DEFINITIONS, ACRONYMS, ABBREVIATIONS

AFR	Air-Fuel Ratio
aTDC	After Top Dead Centre
bTDC	Before Top Dead Centre
CAD	Crank Angle Degree
CD	Combustion Duration n Duration
CO	Carbon Monoxide
CID	Initial Combustion
COV	Coefficient of Variations
CO ₂	Carbon Dioxide
DC	Direct Current
DISI	Direct Injection Spark Ignition
DMF	2,5-Dimethylfuran
FID	Flame Ionization Detector
ETH	Ethanol
GisFC	Gravimetric Indicated Specific Fuel Consumption
HC	Hydrocarbon
HMF	5-hydroxymethylfurfural
HV	Heat of Vaporization
IMEP	Indicated Mean Effective Pressure
isCO	Indicated specific Carbon Monoxide
isHC	indicated specific Hydrocarbon
KLSA	Knock-limited Spark Advance
VisFC	Volumetric Indicated Specific Fuel Consumption
LHV	Lower Heating Value
MBT/KLSA	Maximum Brake Torque/ Knock-Limited Spark Advance

MF	2-Methylfuran
MFB	Mass Fraction Burned
NO _x	Nitrogen Oxides
PID	Proportional Integral Differential
PM	Particulate Matter
RPM	Revolutions per Minute
SI	Spark-ignition
TDC	Top Dead Center
ULG	Gasoline
VVT	Variable Valve Timing

1. Kintisch, E., *Energy research. BP bets big on UC Berkeley for novel biofuels center.* Science, 2007. **315**(5813): p. 747.
2. Atsumi, S., T. Hanai, and J.C. Liao, *Non-fermentative pathways for synthesis of branched-chain higher alcohols as biofuels.* Nature, 2008. **451**(7174): p. 86–89.
3. A. Demirbas and Prog, Energy Combust. **Sci. 33 (1) (2007) 1–18.**
4. Agarwal, A.K., *Bio-fuels (Alcohols and Biodiesel) Applications as fuels for Internal Combustion Engines.* Progress in Energy and Combustion Science, 2007. **33**(3): p. 233-271.
5. Anil Singh Bika, L.F., Prof. David B. Kittelson, *Hydrogen assisted combustion of ethanol in Diesel engines.*
6. Rakopoulos, D.C., et al., *Combustion heat release analysis of ethanol or n-butanol diesel fuel blends in heavy-duty DI diesel engine.* Fuel, 2011. **90**(5): p. 1855-1867.
7. Scania, *New highly efficient diesel-ethanol engine– ready to cut fossil CO₂ emissions by 90%*2007: PRESS info.
8. Zhao, H., et al., *Metal chlorides in ionic liquid solvents convert sugars to 5-hydroxymethylfurfural.* Science, 2007. **316**(5831): p. 1597-600.
9. Roman-Leshkov, Y., et al., *Production of dimethylfuran for liquid fuels from biomass-derived carbohydrates.* Nature, 2007. **447**(7147): p. 982-5.
10. Dumesic, J.A., Y. Roman-Leshkov, and J.N. Chheda, *Catalytic process for producing furan derivatives from carbohydrates in a biphasic reactor,* in *US: World Intellectual Property*2007.

11. Yuriy Román-Leshkov, *Biomass-derived furanic compounds for the production of fuels and chemical intermediates*. 2009.
12. Tian, G., R. Daniel, and H. Xu, *DMF-A New Biofuel Candidate* 2011.
13. Zhong, S.H., et al., *Combustion and Emissions of 2,5-Dimethylfuran in a Direct-Injection Spark-Ignition Engine*. Energy & Fuels, 2010. **24**(5): p. 2891-2899.
14. Daniel, R., et al., *Effect of spark timing and load on a DISI engine fuelled with 2,5-dimethylfuran*. Fuel, 2011. **90**(2): p. 449-458.
15. Wu, X.S., et al., *Dual-injection: The flexible, bi-fuel concept for spark-ignition engines fuelled with various gasoline and biofuel blends*. Applied Energy, 2011. **88**(7): p. 2305-2314.
16. Wu, X.S., et al., *Measurements of Laminar Burning Velocities and Markstein Lengths of 2,5-Dimethylfuran-Air-Diluent Premixed Flames*. Energy & Fuels, 2009. **23**: p. 4355-4362.
17. Tian, G.H., et al., *Laminar Burning Velocities of 2,5-Dimethylfuran Compared with Ethanol and Gasoline*. Energy & Fuels, 2010. **24**(7): p. 3898-3905.
18. Wu, X.S., et al., *Laminar burning characteristics of 2,5-dimethylfuran and iso-octane blend at elevated temperatures and pressures*. Fuel, 2012. **95**(1): p. 234-240.
19. Li, Q., et al., *Laminar flame speeds of DMF-iso-octane-air-N₂/CO₂ mixtures*. . Energy & Fuels, 2012. **25**(2): p. 917-925.
20. Wu, X., et al., *Identification of combustion intermediates in a low-pressure premixed laminar 2,5-dimethylfuran/oxygen/argon flame with tunable synchrotron photoionization*. Combustion and Flame, 2009. **156**(7): p. 1365-76.
21. Thewes, M., et al., *Analysis of the Impact of 2-Methylfuran on Mixture Formation and Combustion in a Direct-Injection Spark-Ignition Engine*. Energy & Fuels, 2011. **25**(12): p. 5549-5561.
22. Agency, C.E.P., *Determination of Hazardous Air Pollutants from Vapor Recovery Processors*, 2001.
23. Heywood, J.B., *Internal combustion engine fundamentals*. McGraw-Hill Book Company 1989.
24. Aleiferis, P.G., et al., *An optical study of spray development and combustion of ethanol, iso-octane and gasoline blends in a DISI engine*, 2008, SAE International.
25. Cairns, A., et al., *A study of gasoline–alcohol blended fuels in an advanced turbocharged DISI engine*, in *SAE International* 2009.
26. Yeliana, et al., *The calculation of mass fraction burn of ethanol–gasoline blended fuels using single and two-zone models*. , 2008, SAE International.
27. Harrington, J.A. and R.C. Shishu, *A single-cylinder engine study of the effects of fuel type, fuel stoichiometry, and hydrogen-to-carbon ratio and CO, NO, and HC exhaust emissions*, 1973, SAE International.
28. Wallner, T. and S.A. Miers, *Combustion Behavior of Gasoline and Gasoline/Ethanol Blends in a Modern Direct-Injection 4-Cylinder Engine*, 2008, SAE International.
29. P., P., et al., *Particulate and Hydrocarbon Emissions from a Spray Guided Direct Injection Spark Ignition Engine with Oxygenate Fuel Blends*, 2007, SAE International.
30. Dale Turnera, et al., *Combustion Performance of Bio-Ethanol at Various Blend Ratios in a Gasoline Direct Injection Engine*. Fuel, 2011. **90**(5): p. 1999-2006.
31. Eastwood, P., *Particulate Emissions from Vehicles* 2007: John Wiley & Sons, Inc.
32. Kittelson, D.B., *Engines and nanoparticles: A review*. Journal of Aerosol Science, 1998. **29**(5-6): p. 575-588.
33. Armas, O., A. Gomez, and C. Mata, *Methodology for measurement of diesel particle size distributions from a city bus working in real traffic conditions*. Measurement Science & Technology, 2011. **22**(10).
34. Yanowitz, J., E. Christensen, and R.L. McCormick, *Utilization of Renewable Oxygenates as Gasoline Blending Components*. National Renewable Energy Laboratory 2012: BiblioGov.